New light Higgs boson and short-baseline neutrino anomalies

J. Asaadi,[1] E. Church,[2] R. Guenette,[3] B. J. P. Jones,[1,*] and A. M. Szelc[4]

[1]*Department of Physics, University of Texas at Arlington, Arlington, Texas 76019, USA*
[2]*Pacific Northwest National Laboratory, P.O. Box 999, Richland, Washington 99352, USA*
[3]*Department of Physics, Harvard University, Cambridge, Massachusetts 02138, USA*
[4]*School of Physics and Astronomy, University of Manchester, Manchester, M13 9PL, United Kingdom*

The low-energy excesses observed by the MiniBooNE experiment have, to date, defied a convincing explanation under the standard model even with accommodation for nonzero neutrino mass. In this paper we explore a new oscillation mechanism to explain these anomalies, invoking a light neutrinophilic Higgs boson, conceived to induce a low Dirac neutrino mass in accord with experimental limits. Beam neutrinos forward scattering off of a locally overdense relic neutrino background give rise to a novel matter effect with an energy-specific resonance. An enhanced oscillation around this resonance peak produces flavor transitions which are highly consistent with the MiniBooNE neutrino- and antineutrino-mode data sets. The model provides substantially improved χ^2 values beyond either the no-oscillation hypothesis or the more commonly explored $3 + 1$ sterile neutrino hypothesis. This mechanism would introduce distinctive signatures at each baseline in the upcoming short-baseline neutrino program at Fermilab, presenting opportunities for further exploration.

I. MOTIVATION

The nature of neutrino mass is widely recognized as one of the most important open theoretical and experimental questions in particle physics. In the Standard Model (SM) particles acquire mass via the Higgs mechanism, and the measured Yukawa couplings of the fermions span from 7×10^{-1} (top quark) to 2×10^{-6} (electron). Under the SM, neutrinos do not couple directly to the Higgs field and so are massless. However, the discovery of neutrino oscillation [1,2] has demonstrated that neutrinos have a tiny but nonzero mass. This mass has current upper limits around $m_\nu \lesssim 2.05$ eV from direct searches [3,4]. Cosmological observations of the cosmic microwave background and baryon acoustic oscillations [5] suggest the sum of neutrino masses is still smaller, $\sum_i m_i < 0.23$ eV. One neutrino mass state may still be massless $m_{\nu 1} \geq 0$, but oscillations [6] place lower limits on the other two masses of $m_a > 8.5$ meV and $m_b > 50$ meV (the identification of subscript a and b with a conventionally numbered mass state depends on the ordering of the neutrino masses). Such small values imply either extremely small Yukawa couplings to the Higgs or a new mechanism for mass generation. Several models have been proposed to try to explain the mass of neutrinos [7–11], many of them predicated on the seesaw mechanism and the generation of a Majorana neutrino mass via the Weinberg operator.

However, the possibility remains that neutrinos are Dirac particles, without a Majorana mass term. The challenge for such models is explaining why the Yukawa coupling to neutrinos is so much smaller than to the other particles [12]. This would be particularly awkward, since the neutrinos are members of SU(2) doublets with the charged leptons, all of which have much larger masses. Admitting Dirac neutrinos thus suggests nontrivial structure in the Higgs sector. This is often codified in two-Higgs-doublet models [13]. In particular, some authors have suggested that new light Higgs fields with a smaller vacuum expectation value (vev) could generate the light neutrino masses, while the standard model Higgs generates the masses of the other fermions [14–17]. In this work we consider possible phenomenological implications of such a scheme. We do not restrict our considerations to any specific embedding within the Standard Model, but rather treat it as a generic consequence of a wider class of models, some examples of which are listed in the above references.

We consider here a minimal model with a single new neutrinophilic Higgs boson that has a standard-model type potential:

$$\mathcal{L}_{\nu\text{Higgs}} = \epsilon^2 \Phi^\dagger \Phi + \zeta (\Phi^\dagger \Phi)^2 \quad \text{with} \quad \epsilon^2 < 0, \zeta > 0, \quad (1)$$

---

*Corresponding author.
ben.jones@uta.edu

generating a new Higgs mass $m_h = \sqrt{2\zeta}v_h > 0$ and a vev $v_h = |\epsilon|/\sqrt{\zeta} > 0$. The masses of the neutrinos are then given by Yukawa couplings to new Higgs:

$$\mathcal{L}_{\nu\text{mass}} = \sum_i (g_i v_h)\bar{\nu}\nu. \tag{2}$$

Both m_h and v_h values are independent free parameters. To generate natural neutrino masses using Yukawa couplings of similar order to those in the standard Higgs sector the vev of the new Higgs field should be in the range 10 meV $< v_h <$ 100 keV. It is worth noting that the "natural" range of Yukawas in this new sector could be entirely unrelated to that in the known Higgs sector, so, as usual, the parameters required for naturalness cannot be stated unambiguously.

The mass of the new boson is an independent and unconstrained parameter which is, in principle, experimentally measurable. If prejudices developed from the SM Higgs sector were directly applicable the Higgs self-coupling ϵ would be $O(1)$, and the new Higgs mass would be of the same order as the new vev. Again, this should only be taken as a rough guide. Finally, we note that the neutrinos in our model are strictly Dirac fermions with no Majorana term present, and we do not rely on a seesaw model to explain their mass scale.

A particularly interesting phenomenological implication of this model is that exchange of this new boson with the cosmic neutrino background (CNB) can, under the circumstances discussed in this paper, generate a resonance observable in neutrino oscillation experiments. In particular, we will show that for a Higgs mass of $O(10$ keV) and a CNB overdensity that is large but within experimental limits, this resonance may be observable in short-baseline neutrino oscillation experiments. In some cases, oscillation signatures very similar to the MiniBooNE low-energy excess may be generated.

II. NEW HIGGS EXCHANGE WITH THE COSMIC NEUTRINO BACKGROUND

We consider a beam of relativistic neutrinos with a narrow momentum spread centered at $\{E, p\}$ acting as test particles. A neutrinophilic Higgs boson introduces a new force between the test particles and other neutrinos but does not couple strongly to other Standard Model particles. These interactions, exhibited between the test particle and the pervasive bath of relic neutrinos produced in the hot big bang, may then generate observable phenomena.

The Higgs couplings to neutrinos are determined by the Yukawa parameters. Were Dirac neutrino masses generated by a standard model Higgs alone, this Yukawa coupling would be of order $10^{-15} < g < 10^{-13}$, and so standard Higgs-to-neutrino interactions would be negligible. A larger contribution comes from Z-boson exchange with the relic
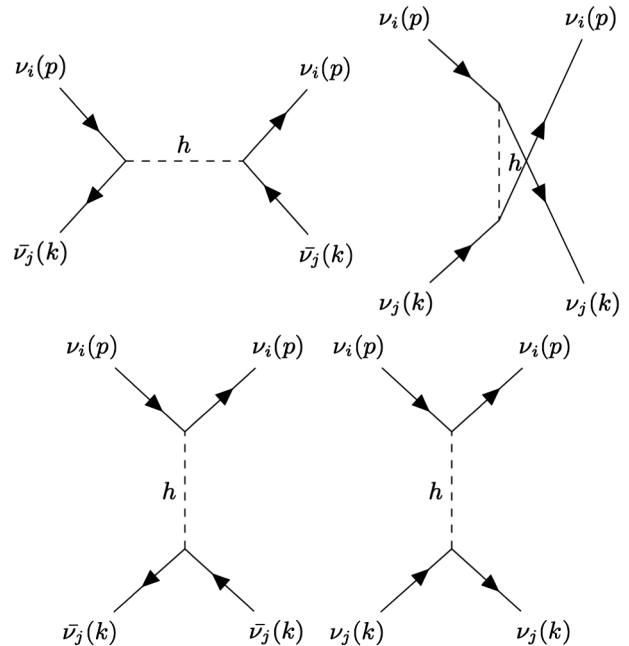

FIG. 1. Feynman diagrams for scattering of neutrinos off CNB neutrinos and antineutrinos. Top row: diagrams 1 and 2. Bottom row: diagrams 3 and 4.

neutrino background, which has been studied in [18], but its effects remain negligible for neutrino experiments.

In our model the vev of the Higgs is much smaller, so the Yukawa coupling used to generate the neutrino masses is large. Under such conditions, coherent forward scattering from the CNB via light Higgs exchange creates a refractive effect. Because this refractive effect depends on the mass composition of the beam, the phase of each mass eigenstate advances at different rates, thus increasing the frequency of neutrino oscillations.

The relevant Feynman diagrams for the interaction of beam neutrinos with CNB neutrinos are shown in Fig. 1. We label each diagram with an amplitude $\mathcal{M}_{ij}^a(p, k)$ where the index a specifies whether a relic ν or $\bar{\nu}$ is involved, p labels the four-momentum of the test neutrino from the beam, decomposed in terms of mass eigenstates i, and k labels the four-momentum of the relic neutrino or antineutrino, decomposed in terms of mass eigenstates j. We describe the calculation for neutrinos, but exactly analogous effects are present for antineutrinos as test particles.

To maintain coherence with the incident beam required for oscillation, we are limited to interactions where the incoming and outgoing momenta and masses of both the test particle and the relic neutrino are unchanged. Given that in our model the mass of the neutrinos is defined by diagonality of the Higgs coupling, it is immediately clear that the first two diagrams only give nonzero contributions when $i = j$.

Applying the Feynman rules, allowing for a finite Higgs width, and assuming the relic neutrinos to be unpolarized, we find the spin-averaged matrix elements:

$$i\langle \mathcal{M}_{ij}^{\bar{\nu},1}\rangle = i\frac{g_i^2[k.p - m_i^2]}{(p+k)^2 - m_h^2 - im_h\Gamma_h}\delta_{ij} \qquad (3)$$

$$i\langle \mathcal{M}_{ij}^{\nu,2}\rangle = i\frac{g_i^2[k.p + m_i^2]}{(p-k)^2 - m_h^2 - im_h\Gamma_h}\delta_{ij} \qquad (4)$$

$$i\langle \mathcal{M}_{ij}^{\bar{\nu},3}\rangle = 2i\frac{g_i^2 g_j^2 \nu_h^2}{m_h^2 - im_h\Gamma_h} \qquad (5)$$

$$i\langle \mathcal{M}_{ij}^{\nu,4}\rangle = -2i\frac{g_i^2 g_j^2 \nu_h^2}{m_h^2 - im_h\Gamma_h}. \qquad (6)$$

To account for the complete refractive effect of the relic background, we must sum over the background momentum and flavor distribution. This distribution is determined by a density function, which in the standard cosmological model is the Fermi-Dirac function, redshifted from decoupling time to a temperature $T \sim 1.95$ K in the present era [19].

In the absence of a chemical potential driving an overdensity of either neutrinos or antineutrinos in the early Universe, $\mu_i = 0$ and the distributions for ν and $\bar{\nu}$ are equivalent. The number density $\langle n_i \rangle$ of all mass states are also expected to be equivalent, with $\langle n_i \rangle = 56$ cm^{-3}, for each flavor, for both neutrinos and antineutrinos.

With equal number densities of relic neutrinos and antineutrinos, the contributions of Feynman diagrams 2 and 3 cancel in the forward scattering amplitude. We assume this case to simplify our calculations. In practice the effects of any asymmetry, if present, would be highly subleading relative to resonant effects in our final expressions.

Small deviations from the baseline model described above are expected, arising from the effects of gravitational clustering for nonrelativistic neutrinos [20,21]. More dramatic clustering effects can, however, arise in the presence of new forces between neutrinos, through the process of "neutrino cloud" formation [22], with enhancements of up to 10^{21} in principle achievable [23,24]. Local overdensities of 10^9 have been discussed in connection with direct relic neutrino detection experiments [25], and are still outside of experimental reach. Independently, large local enhancements of 10^6 have been suggested in [26,27]. Finally, overdensities of 10^{13} have been invoked in order to explain the knee of the cosmic-ray spectrum [28]. In this work we consider the local relic density as a free parameter, and find large observable effects within the range of values previously considered by others.

At temperatures of 2 K, the energies of the relic neutrinos are in the 0.1–1 meV range. Thus all except perhaps the lightest are nonrelativistic, and we can reasonably approximate them to be at rest. The dominant effects in our model will be caused by scattering from the species with the largest Yukawa coupling, that is, the heaviest neutrino mass state. These are necessarily nonrelativistic in the present cosmological era, so we substitute the four vector $k = (m, 0)$ and

replace the sum over the Fermi-Dirac distribution with a simple multiplication by number density. With all these considerations, the only important scattering amplitudes arise from diagrams 1 and 2, each involving a relic neutrino or antineutrino in the same mass eigenstate as the test particle. If we make the assumption that the new boson is truly neutrinophilic, we may substitute for its width:

$$\Gamma = \frac{1}{2}m_h\sum_i g_i^2, \qquad (7)$$

to yield real and imaginary parts of the scattering matrix shown in Eqs. (8) and (9):

$$\text{Re}\langle M\rangle = \delta_{ij}\frac{g_i^2 E}{2m_i^2}\left[\frac{E - E_{\text{res}}^i}{(E - E_{\text{res}}^i)^2 + (\frac{1}{2}E_{\text{res}}^i g_i^2)^2}\right.$$
$$\left. + \frac{-E - E_{\text{res}}^i}{(E + E_{\text{res}}^i)^2 + (\frac{1}{2}E_{\text{res}}^i g_i^2)^2}\right] \qquad (8)$$

$$\text{Im}\langle M\rangle = -\delta_{ij}\frac{g_i^4 E}{4m_i^2}\left[\frac{E_{\text{res}}^i}{(E - E_{\text{res}}^i)^2 + (\frac{1}{2}E_{\text{res}}^i g_i^2)^2}\right.$$
$$\left. + \frac{E_{\text{res}}^i}{(E + E_{\text{res}}^i)^2 + (\frac{1}{2}E_{\text{res}}^i g_i^2)^2}\right]. \qquad (9)$$

In the above equations we introduce an important phenomenological parameter, the resonance energy $E_{\text{res}}^i = m_h^2/2m_i$. It is instructive to consider a more limited model invoking the zero width approximation (ZWA), which involves setting $\Gamma \to 0$ in Eqs. (3) and (4). In practice, this will be a good approximation when the Yukawa couplings are in the range $g \leq 0.1$. In this case, we find

$$\text{Re}\langle M_{\text{ZWA}}\rangle = \delta_{ij}\frac{g_i^2}{4m_i}\left[\frac{-E_{\text{res}}^i}{E^2 - E_{\text{res}}^2}\right] \qquad (10)$$

$$\text{Im}\langle M_{\text{ZWA}}\rangle = 0. \qquad (11)$$

In both the ZWA and finite-width cases, a clear resonance is observed at $E = E_{\text{res}}^i$ for each mass state, corresponding to production of new Higgs bosons at rest in the center of mass frame. Although this resonance only has a small effect in terms of real particle production or scattering, as implied by the $O(g_i^4)$ suppression of $\text{Im}[M]$ and as demanded by the optical theorem, it makes a significant contribution to the real part of the forward scattering amplitude, and thus contributes a large oscillation phase near the resonance.

III. CONNECTION TO NEUTRINO REFRACTIVE PROPERTIES AND OSCILLATIONS

The scattering matrix calculated above has both real and imaginary parts, which contribute to the refractive and

absorptive behaviors of the neutrino beam, respectively. It will be most convenient in what follows to work with the T matrix normalized with single-particle wave functions, rather than the Lorentz-invariant M matrix. These are related by $T = M/4Em_i$.

For relativistic forward scattering we can incorporate the effects of the amplitudes calculated above into the time evolution of the neutrino wave function as

$$\psi' = u_0(p)\text{Exp}[i(p + in_i T_i)x]. \qquad (12)$$

It is easy to verify that neutrino refractive properties reproducing the standard Mikheyev-Smirnov-Wolfenstein (MSW) matter potential are recovered if T is chosen to be that of the weak interactions. In our case, the matrix elements of interest are given instead by Eqs. (3) and (4).

Following the standard derivation of the neutrino oscillation formula, we find the probability for conversion from a neutrino flavor α to neutrino flavor β is given by Eq. (13):

$$P_{\alpha\beta} = \delta_{\alpha\beta} - 4\sum_{i>j}\text{Re}(U_{\alpha i}^*U_{\beta i}U_{\alpha j}U_{\beta j}^*)\sin^2\left[\frac{\Delta_{ij}}{2}L\right]$$

$$+ 2\sum_{i>j}\text{Im}(U_{\alpha i}^*U_{\beta i}U_{\alpha j}U_{\beta j}^*)\sin^2\left[\frac{\Delta_{ij}}{4}L\right] \qquad (13)$$

with $\Delta_{ij} = (p_i - p_j) + n\text{Re}(T_i - T_j)$. Noting that, as usual,

$$p_i - p_j = \left(\sqrt{E^2 - m_i^2} - \sqrt{E^2 - m_j^2}\right) = \frac{\Delta m_{ij}^2}{2E}. \qquad (14)$$

We can substitute for Δ explicitly to find the oscillation phase in this model:

$$\frac{\Delta_{ij}}{2}L = \left(\frac{\Delta m_{ij}^2}{4E} + \frac{1}{2}n\text{Re}[T_i - T_j]\right)L. \qquad (15)$$

When the energy E is very far from the resonant energy E_{res}^i for any mass state, both the new terms are negligible relative to the standard oscillation phase, and we retrieve the usual neutrino oscillation formula. Near resonance for a given mass component m_k, however, new oscillation effects become observable. The case that will be of particular interest to us is the short-baseline regime, where the standard oscillation phase can be neglected and the new terms give the dominant contribution to oscillations.

For simplicity we will neglect CP violation in the following discussion. Allowing for nonzero CP violation introduces further dependencies on the CP phases of the Pontecorvo-Maki-Nakagawa-Sakata (PMNS) matrix which have not been measured, thus introducing extra fit parameters and reducing the predictiveness of this model. These

considerations would modify our results quantitatively by O(1) numbers, though they do not change our primary conclusions.

Under these conditions, near the resonance E_{res}^k and at short baseline, the new oscillation effect takes the form

$$P_{\alpha\beta}\Big|_{L \ll L_{\text{osc}}} = \sin_{\alpha\beta}^2 2\theta \sin^2\left[\frac{1}{2}n\text{Re}[T_k]L\right]. \qquad (16)$$

The effective angle $\sin^2 2\theta_{\mu e}$ is determined entirely from the PMNS matrix, which is assumed to be well measured by off-resonance experiments. Resonances involving mass states lighter than the heaviest one will always be subdominant, due to the reduced Yukawa couplings associated with the smaller masses. Thus the dominant term for oscillation phenomenology in the majority of experimental situations arises for k corresponding to the heaviest neutrino mass state. For the normal mass ordering (NO), this is ν_3, whereas for the inverted ordering (IO) it is ν_2. Thus the combination of mixing angles which determine $\sin^2 2\theta_{\mu e}$ is distinct in these two cases, and given by

$$\sin^2 2\theta_{\mu e}^{\text{NO}} = 4s_{13}^2 s_{23}^2 c_{13}^2(1 - s_{13}^2 s_{23}^2 c_{13}) = 0.033 \qquad (17)$$

$$\sin^2 2\theta_{\mu e}^{\text{IO}} = 4s_{12}c_{13}(c_{12}c_{23} - s_{12}s_{23}s_{13})$$
$$\times [-s_{12}c_{13}(c_{12}c_{23} - s_{12}s_{23}s_{13})] = 0.45. \qquad (18)$$

Following the assumption that only one resonance is accessible in any given experiment, this model, which introduces one new particle, can be parametrized in terms of three phenomenological parameters, Y, E_{res} and g_i, via Eq. (19):

$$P_{\alpha\beta} = \sin_{\alpha\beta}^2 2\theta \sin^2\left[\frac{Y}{2}\left(\frac{E - E_{\text{res}}}{(E - E_{\text{res}})^2 + (\frac{1}{2}E_{\text{res}}g_i^2)^2}\right.\right.$$
$$\left.\left. + \frac{-E - E_{\text{res}}}{(E + E_{\text{res}})^2 + (\frac{1}{2}E_{\text{res}}g_i^2)^2}\right)L\right] \qquad (19)$$

with

$$Y = \frac{g_i^2 n}{8m_i} \quad \text{and} \quad E_{\text{res}} = \frac{m_h^2}{2m_i}. \qquad (20)$$

We can also consider the reduced expression that applies at low values of g_i, in practice less than $g \sim 0.1$, following from the ZWA. Under such an approximation:

$$P_{\alpha\beta}^{\text{ZWA}} = \sin_{\alpha\beta}^2 2\theta \sin^2\left[Y\frac{E_{\text{res}}}{E^2 - E_{\text{res}}^2}L\right]. \qquad (21)$$
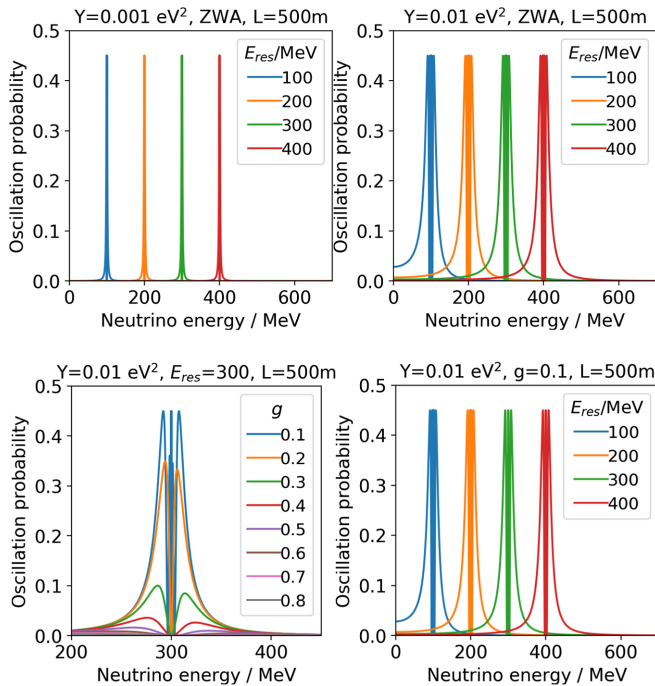
FIG. 2.   Example oscillation probabilities at a 500 m baseline for different values of $E_{\rm res}$, Y, g. Top: Oscillation under the zero width approximation. Bottom: Oscillation for a finite width.

Some examples of the expected oscillation behavior under the ZWA are shown in Fig. 2, where a narrow peak which oscillates rapidly is clearly visible. Figure 2 also shows oscillation probabilities for some finite-width values. For narrow widths, the sharp nature of the resonance remains clear. However, for much larger values of the coupling, the resonance becomes sufficiently wide that nontrivial oscillation structure becomes visible as the oscillation phase changes across the peak. For the majority of the calculations described in this work, the ZWA will suffice. However, we will also briefly explore the consequences of allowing larger couplings and widths using the full model for Eq. (19).

IV. SIGNATURES IN SHORT-BASELINE OSCILLATIONS

The energy-localized oscillation effect described in the previous section is particularly intriguing as a possible explanation for the short-baseline anomalies (see [29] and references therein for a full review). These anomalies suggest oscillations that are inconsistent with the understood three-neutrino paradigm. The leading phenomenological model of these observations invokes a new neutrino mass state with $\Delta m^2 \sim O({\rm eV})^2$ and a corresponding sterile flavor state. There is, however, an ever-growing tension between positive [30,31] and null [32–34] measurements, when world data are interpreted under this model. Here we explore how the new oscillation signature derived in the

previous section may explain the MiniBooNE low-energy excess [30] without significant constraints from other oscillation experiments. We fit the oscillation hypothesis described above in both ZWA and finite width models, and we compare with fits with the "industry standard" $3 + 1$ sterile neutrino model.

Our fit uses the public MiniBooNE data release accompanying [30], and employs the χ^2 minimization recipe provided at [35]. We employ the full MiniBooNE covariance matrix, which simultaneously fits muon- and electron-flavor samples, accounting for cross-correlations and systematic errors in both neutrino and antineutrino modes. We first verified the reproduction of results under the $3 + 1$ model, in excellent agreement with the published MiniBooNE results [30]. The same fit procedure, applied to a different oscillation hypothesis, is used to identify the allowed regions using our model. Following the example of MiniBooNE, we produce allowed regions using neutrino mode data only, using antineutrino mode data only, and using both data sets combined.

For the ZWA we calculate the χ^2 value for points on a grid in $(Y, E_{\rm res})$ for both the normal and inverted mass orderings and then use Wilks theorem to draw 68%, 90%, 95% and 99% confidence intervals in the $(Y, E_{\rm res})$ parameter space. The allowed regions derived when fitting only MiniBooNE neutrino mode data, only antineutrino mode data, and both data sets together are shown in Fig. 3. The allowed regions in both modes are broadly compatible, showing the same two allowed regions overlapping strongly at 90% C.L.

Given the inverted mass ordering, a sharp resonance around 340 MeV describes well the data in both neutrino and antineutrino modes, with χ^2 values that indicate large p-values for the fit. A very low-mass resonance with large amplitude also provides a good fit. For the normal ordering a wide range of resonance energies between 100 MeV and $\sim$350 give very good fits. A selection of favored oscillation hypotheses are shown in Fig. 4.

Relaxing the ZWA and extending the fit into the larger, three-parameter space allows for more flexibility to match the hypothesis at the cost of an extra fitted degree of freedom. Slices at a few selected values of g under both orderings are shown in Fig. 5. Again, there are two allowed regions, but in this case very large values of g tending to favor higher Y are required, as the peak of the resonance becomes suppressed by its finite width.

Given the inverted ordering, the best fit χ^2/DOF (degree of freedom) in the three-parameter fit is 24.6/ 35 DOF, to be compared with 28.9/36 DOF under the ZWA. For the normal ordering, these numbers are 24.6/35 DOF for the three-parameter fit and 24.9/36 DOF for the ZWA. The additional fit parameter provides a modest improvement in the IO case, but not in the NO case. However, as will be discussed in Sec. VI, the large values
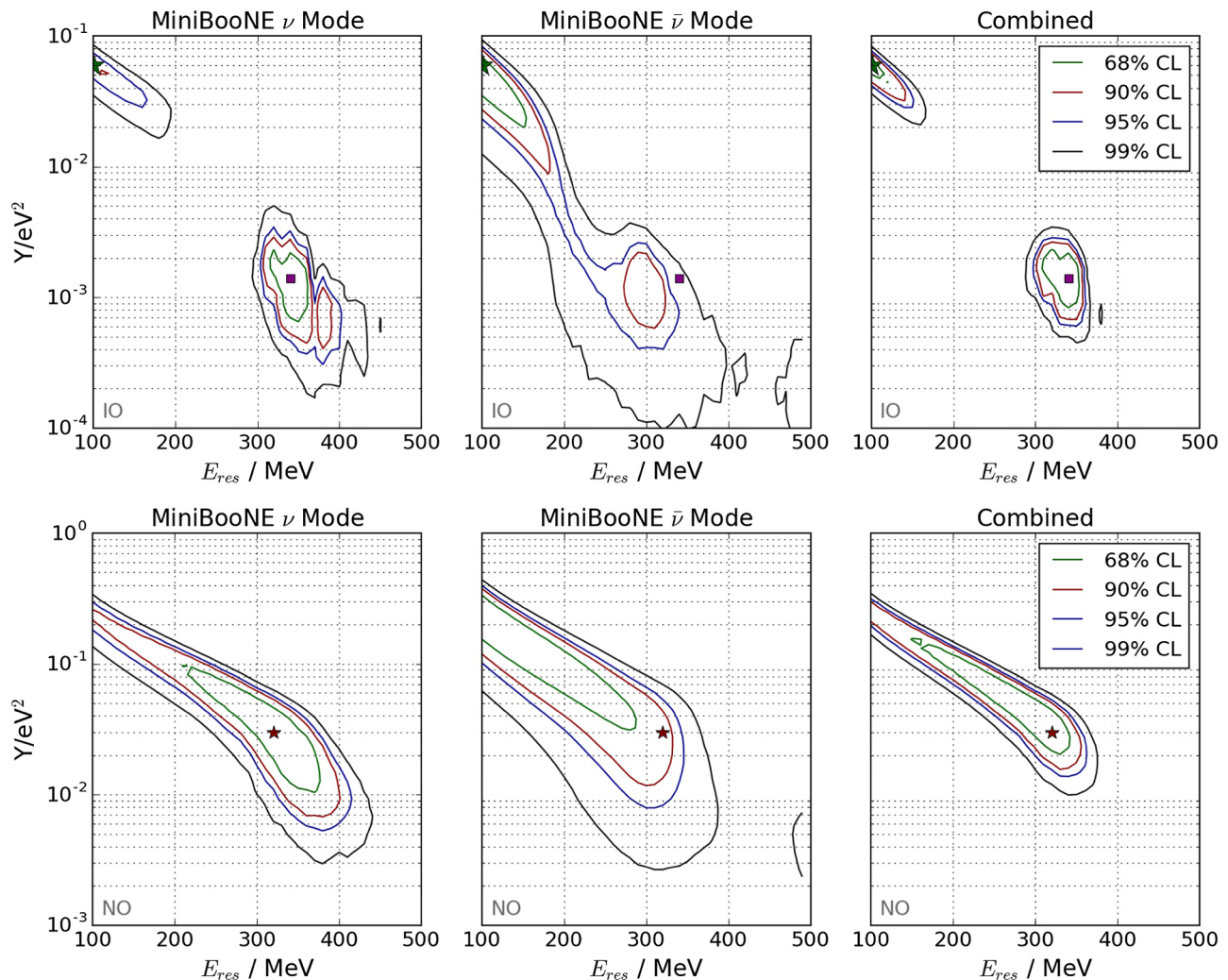
FIG. 3.   Allowed regions of the resonance oscillation effect in the zero width approximation (ZWA) to the MiniBooNE data. Left: fits to neutrino mode only; center: antineutrino mode only; right: combined fit. Top: inverted mass ordering; bottom: normal mass ordering. Stars show the best-fit points in each ordering, and the square shows the local minimum in the high mass island.

of g required in non-ZWA scenarios are difficult to reconcile with limits on secret neutrino interactions from elsewhere [36]. Since the ZWA already gives an excellent fit using one less parameter, we will consider these ZWA best-fit points as the most plausible for further exploration in what follows.

In both ZWA and finite-width models, this new light Higgs hypothesis gives an improvement over the $3 + 1$ model for fitting the MiniBooNE excess. The $3 + 1$ model taken at world-best fit from [37] is only very slightly favored by MiniBooNE data relative to no oscillations, by 3.4 points in $\Delta\chi^2$. The fit to MiniBooNE data only, allowing for parameters disfavored by world data, provides a $\Delta\chi^2$ improvement of 18.6 with 2 DOF. The much larger $\Delta\chi^2$ values for all versions of the neutrinophilic Higgs model (with 2 DOF under the ZWA or 3 DOF with the full finite-width model), of $26 \leq \Delta\chi^2 \leq 31.4$, show that it is a significantly better fit to the MiniBooNE data.

Table I gives a comparison at the best-fit point fitted using combined neutrino and antineutrino data sets, evaluated in neutrino mode, in antineutrino mode, and in both together between various possible models of the excess and the null hypothesis. Our model appears significantly preferred over both the null hypothesis and the sterile neutrino explanation, both at its best-fit point from MiniBooNE only, and at the world-data best fit.

As has been discussed by other authors [39], one should exercise caution in the interpretation of overall χ^2 as a quantitative goodness of fit for each model, since this fit considers both muon- and electron-flavor data simultaneously, only a subset of which is expected to exhibit signal. Fluctuations in the χ^2 at the expected level from nonsignal bins can hide even large anomalies in localized regions. Rather, the key metric for comparing models is $\Delta\chi^2$, which if significantly larger than the number of degrees of freedom in the model, indicates an improvement of compatibility with
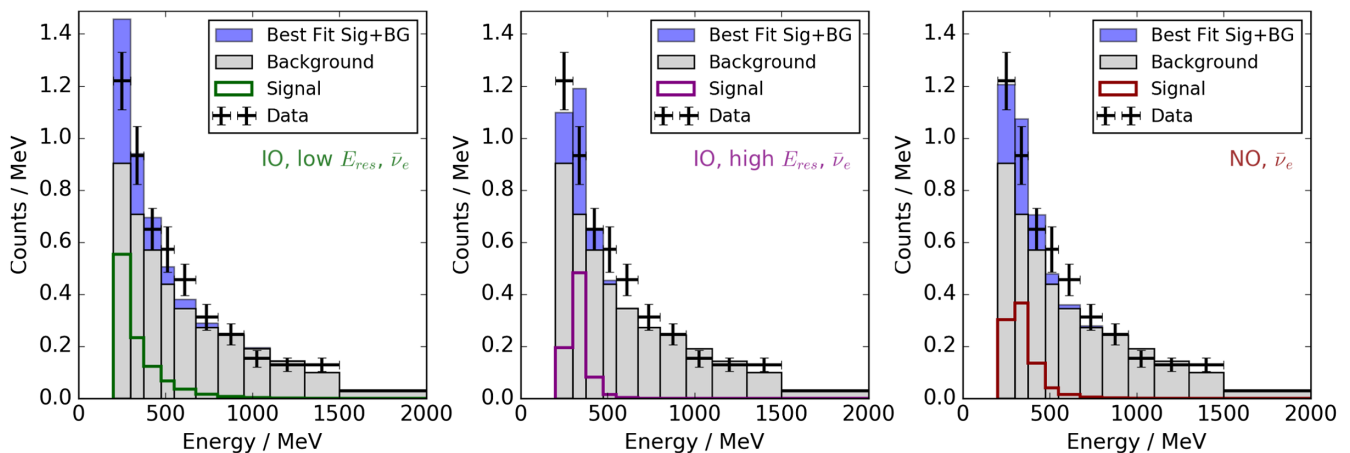
Neutrino Mode
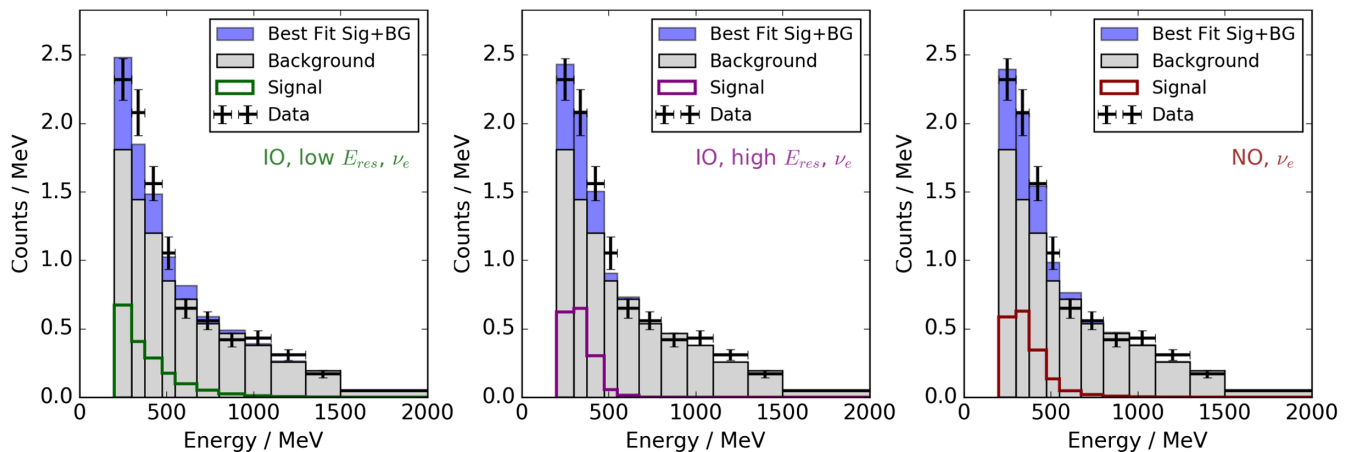
Antineutrino Mode

FIG. 4.   Oscillation spectra in allowed regions under ZWA. Top: neutrino mode. Bottom: antineutrino mode. Left to right: low-mass best fit in inverted ordering ($E_{\mathrm{res}} = 100$ MeV, $Y = 6 \times 10^{-2}$ eV^2); high-mass allowed point in inverted ordering ($E_{\mathrm{res}} = 340$ MeV, $Y = 1.4 \times 10^{-3}$ eV^2); example allowed point in normal ordering ($E_{\mathrm{res}} = 320$, $Y = 3 \times 10^{-2}$ eV^2) region.

data over the null hypothesis. Both $3 + 1$ and light Higgs models, when unconstrained by other oscillation data, provide significant improvements. Furthermore, the light Higgs fits substantially outperform the $3 + 1$ model fits in all favored regions.

V. IMPLICATION FOR FUTURE SHORT-BASELINE NEUTRINO EXPERIMENTS

The short-baseline neutrino (SBN) program at Fermilab [40] has been proposed to directly address the short-baseline oscillation anomalies through the combination of three liquid argon time projection chambers located along the booster neutrino beam. In addition to the oscillation searches from ν_e appearance and ν_μ disappearance, the SBN also offers sensitivity to beyond the standard model searches such as heavy sterile neutrino decay searches [41–43] and sub-GeV dark matter searches running in

beam dump mode [44–47]. These searches are enhanced by the presence of the three detectors because of the baseline dependence of oscillations and the attendant systematic uncertainty reduction afforded by a multi-detector program. The oscillation effect described in this paper would be directly observable by the SBN detectors, and clearly distinguishable from the 3+N sterile neutrino scenario. Figure 6 shows the prediction for the oscillation effect described here at each SBN detector baseline for each of the three favored regions in Fig. 3.

The extrapolated oscillations corresponding to each solution derived from MiniBooNE data show clear and distinctive features in the three SBN detectors. In the case of the low energy IO resonance solution, the oscillation spectrum in each of the detectors has a very different shape. The difference in this spectrum shape provides a powerful handle to identify and classify the effect described here. In the case of the high energy resonance IO solution, the peak
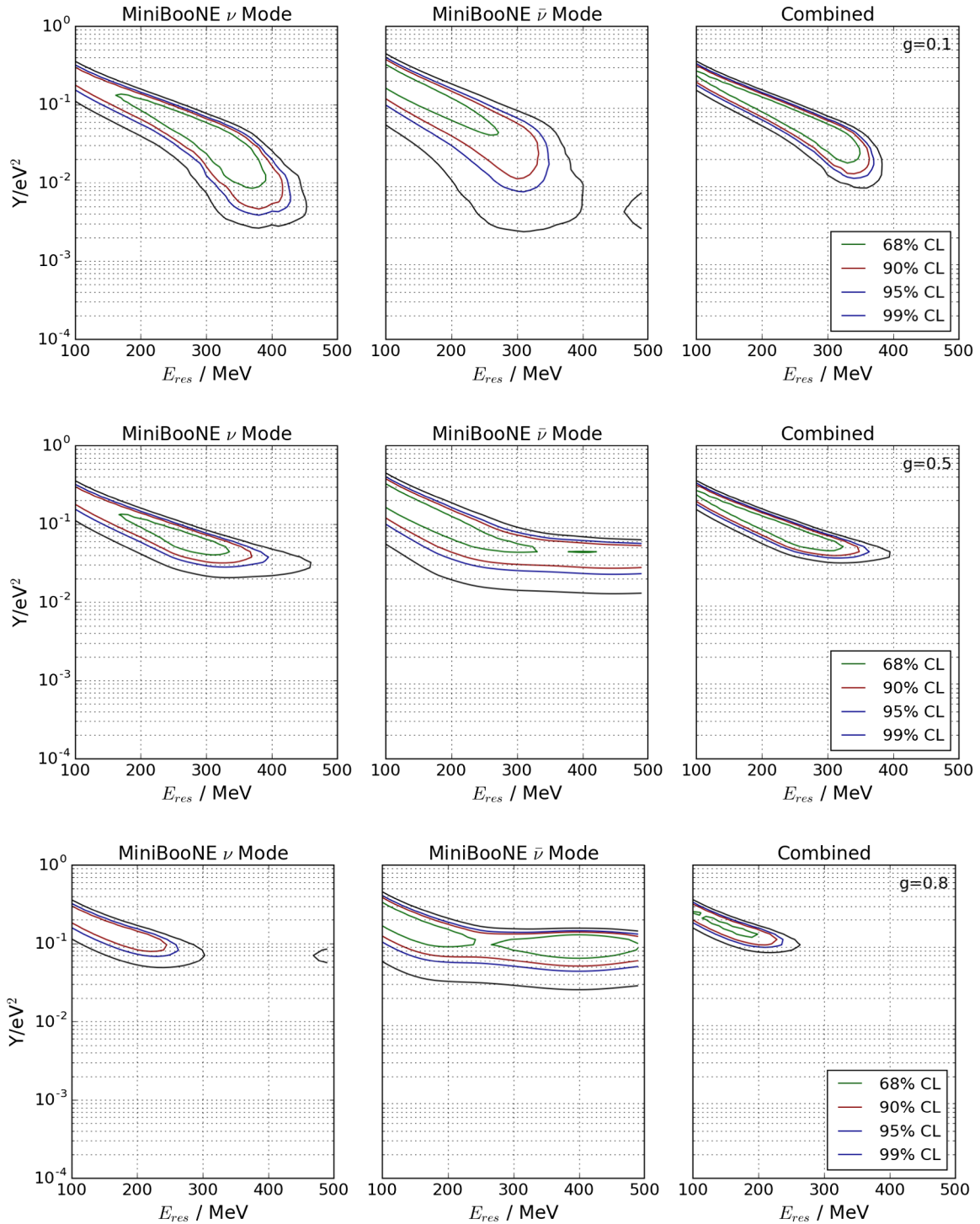
FIG. 5. Slices of the allowed regions at fixed g given the finite width model (3 DOF) under the normal ordering. Left: fits to neutrino mode only; center: antineutrino mode only; right: combined fit.

at 340 MeV in all detectors would be a clear signature of this effect. The NO solution has a smaller amplitude but a nontrivial energy structure at 300 MeV. The energy regime and structure of these effects is ideally suited to exploration at the SBN program, since these detectors are expected to have high efficiency and excellent calorimetric resolution in this energy range. Moreover, the three-detectors configuration allows for the oscillation probability to be mapped as a function of baseline, allowing for detailed exploration of exotic oscillation scenarios such as this one. The combination of three SBN detectors presents the opportunity for a conclusive test of the phenomena

TABLE I. χ^2 values for null hypothesis, the best fit in the $3+1$ model using MiniBooNE and the global fit value from [38], and several of the fit points in the neutrino-Higgs model. In the latter case we consider both the absolute best fit (low mass), the best-fit point in the high mass island for the IO, an allowed value for the NO, and the best fit in the finite width case. These fits use 19 bins in each of neutrino and antineutrino modes (11 ν_e and 8 ν_μ) and data from [30]. The hyphen indicates that this is a point fixed by world data, without additional free fit parameters.

Hypothesis	χ^2_ν	$\chi^2_{\bar{\nu}}$	$\chi^2_\nu + \chi^2_{\bar{\nu}}$	$\Delta\chi^2_{\text{null−bf}}$ (DOF)
No oscillation	24.2	23.5	56.0	N/A
$3+1\ \nu_s$, MB BF	18.8	12.3	37.4	18.6 (2)
$3+1\ \nu_s$, global BF	25.5	19.9	52.6	3.4 (-)
h_ν, ZWA, IO low E_{res}	11.7	13.3	30.0	26.0 (2)
h_ν, ZWA, IO high E_{res}	7.9	20.4	28.9	27.1 (2)
h_ν, ZWA, NO	7.2	15.2	24.9	31.1 (2)
h_ν, IO full	7.8	14.5	24.6	31.4 (3)
h_ν, NO full	7.6	14.6	24.6	31.4 (3)

presented here, as well as other baseline dependent phenomena arising from exotic neutrino oscillation scenarios.

VI. DISCUSSION

We have shown that the MiniBooNE low energy anomalies can be explained using a model with a new, light boson that couples to neutrinos. We demonstrated that the new interaction introduces a resonance in the neutrino oscillation probability due to the forward scatter of neutrinos from an overdense relic neutrino background. The allowed regions in our fits suggest that resonances around $E_{\text{res}} \sim 100$ MeV and $E_{\text{res}} \sim 340$ MeV provide the optimal fit points in the case of the inverted neutrino mass ordering, and for a wide range of masses up to 350 MeV given the normal neutrino mass

ordering. This resonance energy is related to the mass scale of the new boson by $E^i_{\text{res}} = m_h^2/2m_i$.

If the MiniBooNE anomaly is to be explained via this effect, we expect that it must be the heaviest neutrino mass state which is on resonance, in order to avoid conflict with nondetection of larger and higher-energy resonance peaks in other experiments. The mass of this neutrino is constrained from oscillations and cosmology, and the resonance energy leads us to conclude that the mass of this new Higgs boson would be either 6–9 keV in the case of the higher energy class of solutions, or 3–5 keV for the lower energy class.

Of the existing oscillation searches, only the T2K experiment has significant sensitivity in this energy range [48]. Because the maximum oscillation amplitude under the normal mass ordering is small, all hypotheses in the normal ordering scenario are outside the sensitivity of T2K. For the inverted ordering solutions, the effective mixing angle is larger and exploration with T2K is possible. Sensitivity depends on reconstruction efficiency, energy resolution and uncertainty budget in the energy range of interest. These pieces of information are not presently available at the level of detail required to make a careful numerical estimate. However, evaluation of Eq. (16) at 295 km, and comparison to T2K published data [48] strongly suggests that the solutions with large resonance energy, which have smaller Y, will not be excluded within the stated uncertainties. The low mass solutions with larger Y produce a wider resonance at long baselines, which is likely to be at least partially constrained by T2K. Notably, the MINOS [49] and NOνA [50] experiments do not have high enough statistics at low enough energies to address these models with their published analyses, though dedicated searches with cuts optimized for low energy ν_e acceptance may be possible.

For the low energy inverted ordering solution, the other prominent experiment in the appropriate energy
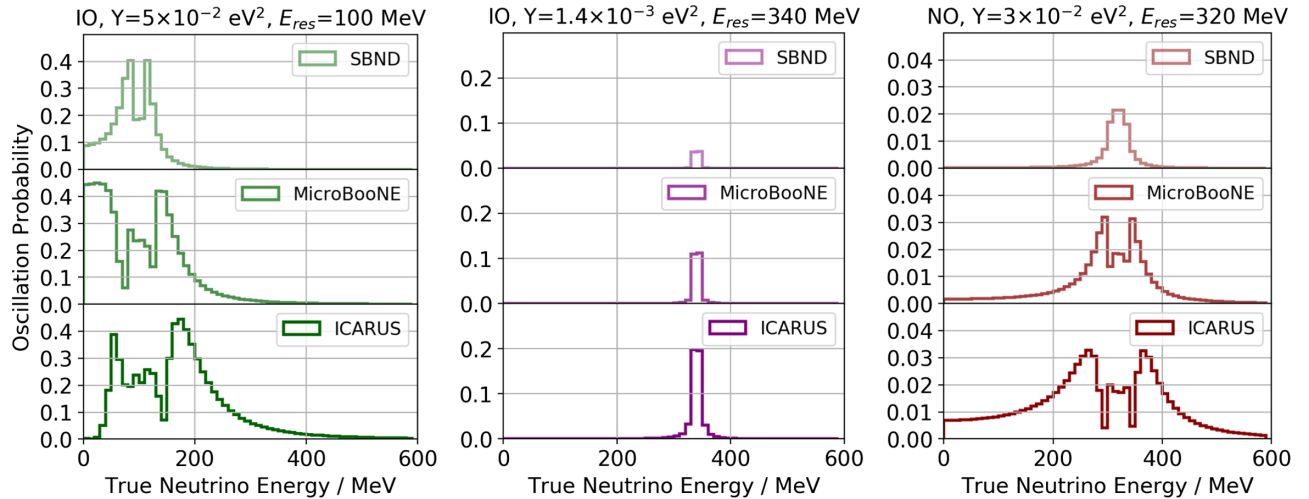

FIG. 6. Predictions for the oscillation probability for the SBN program for the favored high and low energy resonance solutions in IO (left and center) and an example allowed point in the NO (right).

range is LSND [31], which also observes an excess in $\bar{\nu}_e$ appearance. That excess could be explained by this mechanism, though as with any short-baseline oscillation hypothesis, some fine-tuning to maintain consistency with null results from KARMEN [33] would likely be required. A full evaluation of the constraints imposed by world oscillation data would require comprehensive global fits, as have been performed for the $3 + 1$ sterile neutrino hypothesis [38,51,52]. This activity is outside the scope of the present work.

Fitted values of Y of 6×10^{-4} eV^2 and larger are allowed at 90% C.L. The phenomenological parameter Y is related to the coupling strength, neutrino mass and local neutrino overdensity via Eq. (20). Taking the heaviest neutrino mass at its smallest allowed value of 0.05 eV, a relic density $\geq 4 \times 10^{-4}$ eV^3 is implied. This exceeds the standard expected global relic density by a factor of order 10^8. This is a large value, but it remains outside of direct experimental limits. It is also comfortably within the range of densities which may occur under neutrino cloud formation scenarios due to new forces between neutrinos [22], which may be as large as 10^{21} [24]. Such levels of overdensity should be observable by future proposed experiments [53].

Constraints on "secret" neutrino interactions (compiled in [36]) may further bound the range of values for n that are consistent with our fitted parameters. These constraints fall into two broad classes: direct limits on g_i from particle decay widths [54,55], and limits from absorption or down-scattering of neutrinos traveling over astronomical baselines proportionally to $\eta = g_i^4 n$ [36,56]. Since the refractive mechanism described here depends on $g_i^2 n = \eta/g^2$ both are naturally evaded with a suitably large local overdensity and small g_i.

Constraints on secret neutrino interactions from meson decays are derived experimentally in terms of coupling constants to neutrino flavor eigenstates, whereas here we consider mass-diagonal couplings. Using the appropriate mixing parameters and masses it is possible to reexpress the limits from [55] in this space. Figure 7 shows the 90% C.L. upper limit on g, the coupling to the heaviest mass state under each ordering assumption, given a massless lightest neutrino.

The absorption strength of propagating neutrinos on the relic neutrino background can be related to the imaginary part of the forward scattering amplitude via the optical theorem. The heaviest mass states experience the largest couplings and are more strongly absorbed, and conversely, a lightest neutrino with an arbitrarily small mass would not absorb at all. For this reason, objects where the source neutrino luminosity is not known to better than a factor ~ 3, such as supernova 1987A [56] or high energy astrophysical accelerators [36], cannot be used to meaningful limits on this mechanism.

For solar neutrinos, on the other hand, the initial flux is well predicted by the standard solar model (SSM) [57,58].
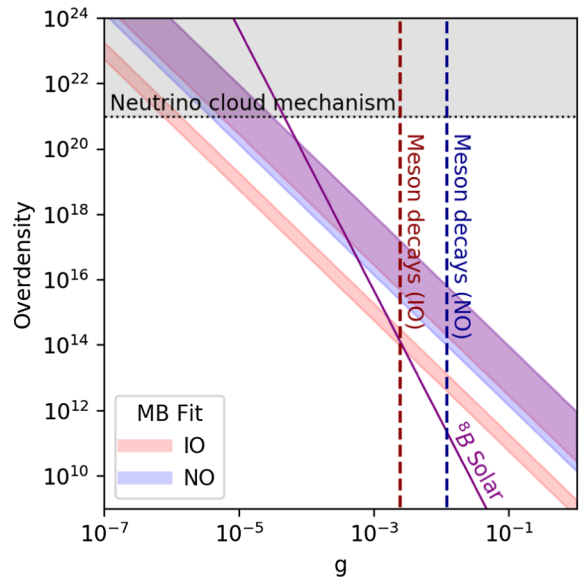

FIG. 7.   The 90% C.L. best-fit regions expressed in terms of coupling strength to the heaviest neutrino state and CNB over-density, compared to various 90% C.L. experimental limits described in the text.

The ^{8}B flux in particular has been measured to 3% precision ($\Phi_B = 5.05^{+0.19}_{-0.20} \times 10^6$ cm^{-2} s^{-1}) [59], and is found to be consistent with predictions of the SSM within uncertainty ($\Phi_B = 5.69 \pm 0.9 \times 10^6$ cm^{-2} s^{-1}) [6]. This implies a constraint on the surviving fraction of 0.89 ± 0.16. ^{8}B neutrinos exit the sun in mass eigenstate m_2 due to adiabatic MSW conversion, and hence an upper limit can be placed on g_2 that can be reexpressed in terms of g given an assumption about the absolute neutrino mass scale. The 90% C.L. limit given a massless lightest neutrino is shown in Fig. 7.

There are also possible implications of a new light scalar for cosmology [43,60,61]. Naively this particle contributes $\Delta N_{\text{eff}} = 4/7$ of a neutrino-equivalent degree of freedom in the early Universe. This is consistent with measurements of big bang nucleosynthesis at the 1.5σ level [6,62–64]. The Planck [5] determination of $N_{\text{eff}} = 3.04 \pm 0.18$ from the CMB, taken at face value, would appear to be a stronger constraint. However, this measurement is strongly correlated with the measured Hubble constant, which is in significant tension with direct determinations [65–67]. Fixing the value of H_0 to that measured elsewhere would substantially weaken the constraint on N_{eff}, pulling it to higher values, and thus drawing the robustness of this constraint into question.

Although preliminary indications suggest that the constraints from cosmology are not overly severe, the extent to which this particle is in equilibrium, and the impact of its possible late-era phase transition, may complicate the simple interpretation of these constraints given above. We thus defer a full account of cosmological implications of this model to future work.

VII. CONCLUSIONS

In this paper we have presented the phenomenological implications of a light, neutrinophilic Higgs boson, motivated as a mechanism to generate neutrino mass. A resonance effect from a neutrino beam interacting with an overdense relic neutrino background is explored that can provide an alternate explanation to short-baseline oscillation anomalies. This model provides a good fit to the MiniBooNE low-energy excess and illustrates an interesting class of new oscillation phenomena. This may provide a promising direction for new physics searches at the Fermilab Short-Baseline Neutrino program and beyond.

ACKNOWLEDGMENTS

[1] A. B. McDonald, Rev. Mod. Phys. **88,** 030502 (2016).
[2] T. Kajita, Rev. Mod. Phys. **88,** 030501 (2016).
[3] C. Kraus *et al.*, Eur. Phys. J. C **40,** 447 (2005).
[4] V. N. Aseev *et al.* (Troitsk Collaboration), Phys. Rev. D **84,** 112003 (2011).
[5] P. A. R. Ade *et al.* (Planck Collaboration), Astron. Astrophys. **594,** A13 (2016).
[6] C. Patrignani *et al.* (Particle Data Group), Chin. Phys. C **40,** 100001 (2016).
[7] D. Chang and R. N. Mohapatra, Phys. Rev. D **32,** 1248 (1985).
[8] P. Minkowski, Phys. Lett. B **67,** 421 (1977).
[9] M. Gell-Mann, P. Ramond, and R. Slansky, *Supergravity*, edited by P. van Nieuwenhuizen and D. Z. Freedman (North-Holland, Amsterdam, 1979).
[10] M. Fukugita and T. Yanagida, Phys. Lett. B **174,** 45 (1986).
[11] R. N. Mohapatra and G. Senjanović, Phys. Rev. D **23,** 165 (1981).
[12] J. F. Donoghue, Annu. Rev. Nucl. Part. Sci. **66,** 1 (2016).
[13] G. C. Branco, P. M. Ferreira, L. Lavoura, M. N. Rebelo, M. Sher, and J. P. Silva, Phys. Rep. **516,** 1 (2012).
[14] F. Wang, W. Wang, and J. M. Yang, Europhys. Lett. **76,** 388 (2006).
[15] S. Gabriel and S. Nandi, Phys. Lett. B **655,** 141 (2007).
[16] S. Baek and T. Nomura, J. High Energy Phys. 03 (2017) 059.
[17] S. M. Davidson and H. E. Logan, Phys. Rev. D **80,** 095008 (2009).
[18] J. S. Diaz and F. R. Klinkhamer, Phys. Rev. D **93,** 053004 (2016).
[19] C. Giunti and C. W. Kim, *Fundamentals of Neutrino Physics and Astrophysics* (Oxford University Press, New York, 2007).
[20] A. Ringwald and Y. Y. Y. Wong, J. Cosmol. Astropart. Phys. 12 (2004) 005.
[21] P. F. de Salas, S. Gariazzo, J. Lesgourgues, and S. Pastor, J. Cosmol. Astropart. Phys. 09 (2017) 034.
[22] G. J. Stephenson, Jr., J. T. Goldman, and B. H. J. McKellar, Int. J. Mod. Phys. A **13,** 2765 (1998).
[23] B. H. J. McKellar, M. Garbutt, G. J. Stephenson, Jr., and J. T. Goldman, Lepton and photon interactions at high energies, in *Proceedings, 20th International Symposium, LP 2001, Rome, Italy, 2001* [arXiv:hep-ph/0106123].
[24] T. Goldman (private communication).
[25] A. Kaboth, J. A. Formaggio, and B. Monreal, Phys. Rev. D **82,** 062001 (2010).
[26] A. Faessler, R. Hodak, S. Kovalenko, and F. Simkovic, Int. J. Mod. Phys. E **26,** 1740008 (2017).
[27] R. Lazauskas, P. Vogel, and C. Volpe, J. Phys. G **35,** 025001 (2008).
[28] W.-Y. P. Hwang and B.-Q. Ma, New J. Phys. **7,** 41 (2005).
[29] K. N. Abazajian *et al.*, arXiv:1204.5379.
[30] A. A. Aguilar-Arevalo *et al.* (MiniBooNE Collaboration), Phys. Rev. Lett. **110,** 161801 (2013).
[31] C. Athanassopoulos *et al.* (LSND Collaboration), Phys. Rev. Lett. **77,** 3082 (1996).
[32] M. G. Aartsen *et al.* (IceCube Collaboration), Phys. Rev. Lett. **117,** 071801 (2016).
[33] K. Eitel *et al.* (KARMEN Collaboration), *Proceedings, International Conference on Neutrino Physics and Astrophysics (Neutrino'98): Takayama, Japan, 1998* [*Nucl. Phys. Proc. Suppl.* 77, 212 (1999)].
[34] P. Adamson *et al.* (MINOS Collaboration), arXiv:1710.06488.
[35] A. A. Aguilar-Arevalo *et al.* (MiniBooNE Collaboration), Instructions on how to use May 2009 MiniBooNE public data for muon-to-electron neutrino oscillation fits, https://www-boone.fnal.gov/for_physicists/data_release/lowe/miniboone_may09publicdata_instructions.pdf.
[36] K. C. Y. Ng and J. F. Beacom, Phys. Rev. D **90,** 065035 (2014).
[37] G. H. Collin, C. A. Argelles, J. M. Conrad, and M. H. Shaevitz, Phys. Rev. Lett. **117,** 221801 (2016).
[38] G. H. Collin, C. A. Argelles, J. M. Conrad, and M. H. Shaevitz, Nucl. Phys. **B908,** 354 (2016).
[39] M. Maltoni and T. Schwetz, Phys. Rev. D **68,** 033020 (2003).
[40] R. Acciarri *et al.*, arXiv:1503.01520.

[41] S. N. Gninenko, Phys. Rev. Lett. **103**, 241802 (2009).

[42] S. N. Gninenko, Phys. Rev. D **85**, 051702 (2012).

[43] A. D. Dolgov, S. H. Hansen, S. Pastor, S. T. Petcov, G. G. Raffelt, and D. V. Semikoz, Nucl. Phys. **B632**, 363 (2002).

[44] B. Batell, M. Pospelov, and A. Ritz, Phys. Rev. D **80**, 095024 (2009).

[45] P. deNiverville, M. Pospelov, and A. Ritz, Phys. Rev. D **84**, 075020 (2011).

[46] P. deNiverville, D. McKeen, and A. Ritz, Phys. Rev. D **86**, 035022 (2012).

[47] A. A. Aguilar-Arevalo et al. (MiniBooNE-DM Collaboration), Phys. Rev. Lett. **118**, 221803 (2017).

[48] K. Abe et al. (The T2K Collaboration), Phys. Rev. D **96**, 092006 (2017).

[49] P. Adamson et al. (MINOS Collaboration), Phys. Rev. Lett. **110**, 171801 (2013).

[50] P. Adamson et al. (NOνA Collaboration), Phys. Rev. Lett. **118**, 231801 (2017).

[51] J. Kopp, P. A. N. Machado, M. Maltoni, and T. Schwetz, J. High Energy Phys. 05 (2013) 050.

[52] S. Gariazzo, C. Giunti, M. Laveder, Y. F. Li, and E. M. Zavanin, J. Phys. G **43**, 033001 (2016).

[53] S. Betts et al., arXiv:1307.4738.

[54] M. S. Bilenky and A. Santamaria, in Neutrino mixing. Festschrift in honour of Samoil Bilenky's 70th birthday,

in Proceedings of the International Meeting, Turin, Italy, 1999, pp. 50–61 [arXiv:hep-ph/9908272].

[55] A. P. Lessa and O. L. G. Peres, Phys. Rev. D **75**, 094001 (2007).

[56] E. W. Kolb and M. S. Turner, Phys. Rev. D **36**, 2895 (1987).

[57] J. N. Bahcall, A. M. Serenelli, and S. Basu, Astrophys. J. **621**, L85 (2005).

[58] J. N. Bahcall and A. M. Serenelli, Astrophys. J. **626**, 530 (2005).

[59] B. Aharmim et al. (SNO Collaboration), Phys. Rev. C **81**, 055504 (2010).

[60] S. Hannestad and J. Madsen, Phys. Rev. D **52**, 1764 (1995).

[61] S. Hannestad and G. Raffelt, Phys. Rev. D **72**, 103514 (2005).

[62] A. Peimbert, M. Peimbert, and V. Luridiana, Rev. Mex. Astron. Astrofis. **52**, 419 (2016).

[63] E. Aver, K. A. Olive, and E. D. Skillman, J. Cosmol. Astropart. Phys. 07 (2015) 011.

[64] Y. I. Izotov, T. X. Thuan, and N. G. Guseva, Mon. Not. R. Astron. Soc. **445**, 778 (2014).

[65] G. Efstathiou, Mon. Not. R. Astron. Soc. **440**, 1138 (2014).

[66] A. G. Riess et al. (Supernova Search Team), Astron. J. **116**, 1009 (1998).

[67] W. L. Freedman, B. F. Madore, V. Scowcroft, C. Burns, A. Monson, S. E. Persson, M. Seibert, and J. Rigby, Astrophys. J. **758**, 24 (2012).